

Federated Modality-specific Encoders and Multimodal Anchors for Personalized Brain Tumor Segmentation

Qian Dai^{1,*}, Dong Wei^{2,*}, Hong Liu^{2,3,*}, Jinghan Sun^{2,3}, Liansheng Wang^{1,†}, Yefeng Zheng²

¹School of informatics, Xiamen University, Xiamen, China

²Jarvis Research Center, Tencent Youtu Lab / Tencent Healthcare (Shenzhen) Co., Ltd., Shenzhen, China

³School of Medicine, Xiamen University, Xiamen, China

{daiqian,liuhong,jhsun}@stu.xmu.edu.cn, lswang@xmu.edu.cn, {donwei,yefengzheng}@tencent.com,

Abstract

Most existing federated learning (FL) methods for medical image analysis only considered intramodal heterogeneity, limiting their applicability to multimodal imaging applications. In practice, it is not uncommon that some FL participants only possess a subset of the complete imaging modalities, posing inter-modal heterogeneity as a challenge to effectively training a global model on all participants' data. In addition, each participant would expect to obtain a personalized model tailored for its local data characteristics from the FL in such a scenario. In this work, we propose a new FL framework with federated modality-specific encoders and multimodal anchors (FedMEMA) to simultaneously address the two concurrent issues. Above all, FedMEMA employs an exclusive encoder for each modality to account for the inter-modal heterogeneity in the first place. In the meantime, while the encoders are shared by the participants, the decoders are personalized to meet individual needs. Specifically, a server with full-modal data employs a fusion decoder to aggregate and fuse representations from all modality-specific encoders, thus bridging the modalities to optimize the encoders via backpropagation reversely. Meanwhile, multiple anchors are extracted from the fused multimodal representations and distributed to the clients in addition to the encoder parameters. On the other end, the clients with incomplete modalities calibrate their missing-modal representations toward the global full-modal anchors via scaled dot-product cross-attention, making up the information loss due to absent modalities while adapting the representations of present ones. FedMEMA is validated on the BraTS 2020 benchmark for multimodal brain tumor segmentation. Results show that it outperforms various up-to-date methods for multimodal and personalized FL and that its novel designs are effective. Our code is available.

Introduction

Federated learning (FL) enables participants to collaboratively train a global model on their collective data without breaching privacy (Li et al. 2020). The decentralized mechanism makes it particularly suitable for privacy-sensitive application scenarios such as medical image analysis (Kaissis et al. 2020; Adnan et al. 2022; Bercea et al. 2021; Yan et al.

*These authors contributed equally.

†Corresponding author.

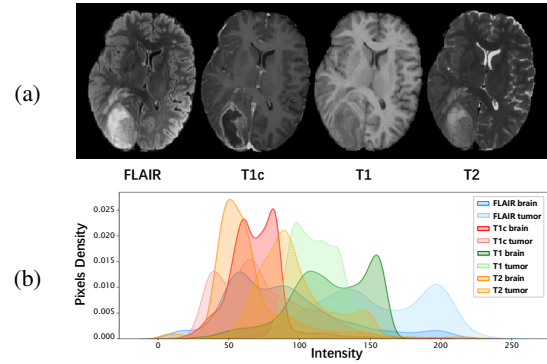


Figure 1: (a) Example images of the four modalities in BraTS 2020 (Menze et al. 2014). (b) Histograms of the brain and tumor pixels for the four modalities.

2021, 2020). However, most FL methods for medical image analysis only considered intramodal heterogeneity, limiting their applicability to multimodal imaging in practice.

One such application is brain tumor segmentation in multi-parametric magnetic resonance imaging (MRI) (Iv et al. 2018). Specifically, four MRI modalities (in this work, we refer to MRI sequences as modalities following literature (Dorent et al. 2019; Menze et al. 2014; Shen and Gao 2019; Zhou et al. 2021)) are commonly used to provide complementary information and support sub-region analysis: T1-weighted (T1), contrast-enhanced T1-weighted (T1c), T2-weighted (T2), and T2 fluid attenuation inversion recovery (FLAIR), where the first two highlight tumor core and the last two highlight peritumoral edema (Fig. 1(a)). When applying FL to such multimodal applications in practice, it is not uncommon that some participant institutes only possess a subset of the full modalities due to different protocols practiced, presenting a new challenge with the *inter-modal heterogeneity* (Fig. 1(b)) across the participants of FL. In such a scenario, there can be two objectives for FL: 1) collectively training an optimal global model for full-modal input, and 2) obtaining a personalized model for each participant (Chen and Zhang 2022; Wang et al. 2019), adapted for its data characteristics, and more importantly, better than trained locally without FL. To our knowledge, these two objectives were rarely considered together in FL for medical image analysis.

In this paper, we propose a new FL framework with federated modality-specific encoders and multimodal anchors (FedMEMA) for brain tumor segmentation. Above all, to handle the distinctively heterogeneous MRI modalities, FedMEMA employs an exclusive encoder for each modality to allow a great extent of parameter specialization. In the meantime, while the encoders are shared between the server and clients, the decoders are personalized to cater to individual participants. Specifically, a multimodal fusion decoder on the server (i.e., a participant with full-modal data) aggregates and fuses representations from the encoders to bridge the distribution gaps between modalities and reversely optimizes the encoders via backpropagation. Meanwhile, multiple anchors are extracted from the fused multimodal representations and distributed to the clients in addition to the encoder parameters. On the other end, the clients with incomplete modalities calibrate their local missing-modal representations toward the global full-modal anchors via the scaled dot-product attention mechanism (Vaswani et al. 2017) to make up the information loss due to absent modalities and adapt representations of present ones. To this end, we simultaneously obtain an optimal server model (for full-modal input) and personalized client models (for specific missing-modal input) from FL without sharing privacy-sensitive information.

In summary, our contributions are as follows:

- We bring forward the inter-modal heterogeneity problem due to missing modalities in FL for medical image analysis and aim to obtain an optimal full-modal server model and personalized missing-modal client models simultaneously with a novel framework coined FedMEMA.
- To tackle the inter-modal heterogeneity, we propose to employ a federated encoder exclusive for each modality followed by a server-end multimodal fusion decoder. Meanwhile, personalized decoders are employed for the clients to allow simultaneous personalization.
- In addition, we propose to extract and distribute multimodal representations from the server to the clients for local calibration of modality-specific features.
- Last but not least, we further enhance the calibration with multi-anchor representations.

Experimental results on the public BraTS 2020 benchmark show that our method achieves superior performance for both the server and client models to existing FL methods and that its novel designs are effective.

Related Work

Brain Tumor Segmentation with Multimodal MRI: Multimodal MRI is the current standard of care for clinical imaging of brain tumors (Iv et al. 2018). Segmentation and associated volume quantification of heterogeneous histological sub-regions are valuable to the diagnosis/prognosis, therapy planning, and follow-up of brain tumors (Menze et al. 2014). In recent years, deep neural networks (DNNs) significantly advanced state-of-the-art of brain tumor segmentation with multimodal MRI (Chen et al. 2020; Chen, Ding, and Liu 2019; Ding et al. 2020; Myronenko 2018;

Zhou et al. 2020). However, these methods were optimized for ideal scenarios where the complete set of modalities was present. In practice, scenarios of missing one or more modalities commonly occur due to image corruption, artifacts, acquisition protocols, allergy to contrast agents, or cost. Therefore, many efforts have been made to accommodate the practical scenarios of missing modalities (Hu et al. 2020; Wang et al. 2021; Ding, Yu, and Yang 2021; Azad, Khosravi, and Merhof 2022). These methods successfully improved DNNs’ feature representation capability against missing modalities—however, only in the centralized setting, limiting their efficacy in privacy-sensitive settings. In this work, we aim to address the missing-modal problem in the FL setting and eliminate the privacy issue.

Multimodal FL with Data Heterogeneity: Data heterogeneity is a primary challenge in FL (McMahan et al. 2017). Personalized FL (Tan et al. 2022a) proposed to adapt the global model locally on clients’ data to address this issue. However, it did not consider the heterogeneity due to multimodal data. We are aware of several works for multimodal FL in the natural image domain. Xiong et al. (2022) proposed a co-attention mechanism to fuse the complementary information of different modalities, yet requiring all clients to have access to the same set of modalities. FedIoT (Zhao, Barnaghi, and Haddadi 2022) employed cross-modal autoencoders to learn multimodal representations in an unsupervised manner. However, both methods (Xiong et al. 2022; Zhao, Barnaghi, and Haddadi 2022) only obtained a single global classifier without catering to the personalized needs of modal-heterogeneous clients. Yu et al. (2023) proposed a cross-modal contrastive representation ensemble between the server and modal-heterogeneous clients by sharing a multimodal dataset, which may be unacceptable in strict privacy restrictions like healthcare. In contrast, our framework optimizes a global model for full-modal input and simultaneously customizes a personalized model for each client’s hetero-modal input. It also maintains FL’s data privacy by transmitting population-wise abstracted prototypes instead of image-wise features.

In medical image analysis, heterogeneity issues in multimodal FL have yet to be thoroughly discussed. FedNorm (Bernecker et al. 2022) adapted the normalization parameters for different modalities while sharing common backbone parameters for CT- and MRI-based liver segmentation. Yet, our experiments suggest that merely specializing in normalization parameters is insufficient to deal with the inter-modal heterogeneity in multimodal brain tumor segmentation. In this work, we propose to handle the heterogeneity with modality-specific encoders to allow a greater extent of parameter specialization, followed by a multimodal fusion decoder to aggregate and fuse representations from the encoders and bridge the inter-modal distribution gaps.

Method

Problem Definition: Let us denote the full set of modalities by $M = \{T1, T1c, T2, FLAIR\}$ and a full-modal input by $X_M \in \mathbb{R}^{|M| \times D \times H \times W}$, where D , H , and W are the depth, height, and width of the volume, respectively. We

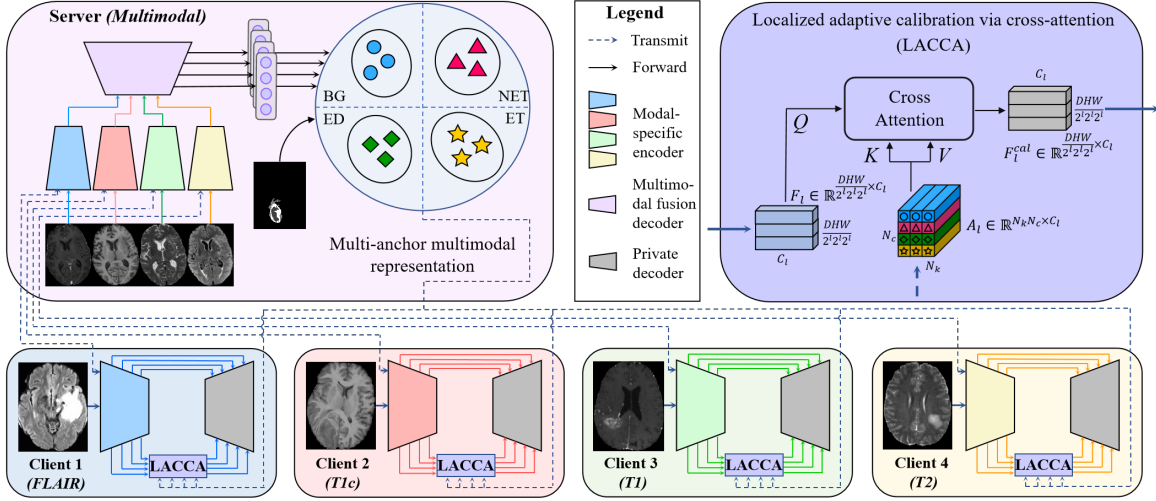


Figure 2: Overview of the proposed FedMEMA framework. FedMEMA employs a federated encoder exclusive for each modality followed by a server-end multimodal fusion decoder. Meanwhile, personalized decoders are used for the clients to allow simultaneous personalization. In addition, multi-anchor multimodal representations are extracted from the server and distributed to the clients for localized adaptive calibration of modality-specific features via cross-attention. ED: edema, ET: enhancing tumor, NET: necrotic and non-enhancing tumor core, and BG: background.

consider a heterogeneous FL setting where a server with access to a set of full-modal data $\{(X_M, Y)\}$ coordinates several clients with access to data of incomplete modalities (“missing-modal”), where $Y \in \mathbb{R}^{N_c \times D \times H \times W}$ is the segmentation mask and N_c is the number of target classes. In practice, the server may be a major regional hospital, whereas the clients may be smaller local health units. In this work, we mainly address the *extreme and most challenging case* of monomodal clients, i.e., each client houses data of a specific modality denoted by $\{(X_m, Y)\}$, where $X_m \in \mathbb{R}^{1 \times D \times H \times W}$, for a pioneer and exploratory methodology development (some preliminary results in the more common settings of multimodal clients are provided in the supplementary material). Furthermore, we mainly consider the horizontal FL setting where 1) each client has different patients, or 2) a client may share some patients with another, i.e., various clients may have different modalities of the same patients. The latter scenario is practical as a patient may have different imaging studies at different hospitals within a district. However, considering the privacy issue, the clients do not know whether or which of their data overlaps with others’.

This work aims to train, via FL, not only an optimal global model that works well with full-modal data but also optimal personalized models that work well in specific missing-modal situations for the clients. The latter is practically meaningful as it is usually difficult for a local health unit to upgrade its imaging protocol quickly, yet still look forward to training an optimal model for its current protocol by participating in the FL.

Framework Overview: Without loss of generality, we use four clients, each with data of a mutually different modality, for method description. As shown in Fig. 2, the server

has four modality-specific encoders (one for each modality) and a modal fusion decoder, whose fused features are clustered to produce multimodal anchors. Meanwhile, each client has a modality-specific encoder for local data modality and a private decoder. Additionally, a localized adaptive calibration via cross-attention (LACCA) module calibrates the clients’ missing-modal representations toward the server’s multimodal anchors.

FL with Modality-specific Encoders: In classical FedAvg (McMahan et al. 2017), the server and clients usually share the same network architecture, where the server aggregates and averages the network parameters of the clients and then distributes the averaged parameters back to the clients in a straightforward manner. However, due to the high heterogeneity among the multimodal MRI data (see Fig. 1), our problem setting becomes challenging for this paradigm. Instead, we propose federated modality-specific encoders to handle the distinctively heterogeneous imaging modalities. On the one hand, we adopt an architecture with late fusion strategy (Ding, Yu, and Yang 2021) to compose the global model on the server, including a modality-specific encoder E_m (parameterized by W_m^s) for each modality, a fusion decoder D_M for multimodal feature aggregation and fusion, and a regularizer (not shown in Fig. 2 for simplicity). The regularizer is a straightforward auxiliary segmentation decoder shared by all modality-specific encoders. It regularizes the encoders to learn the same discriminative features by forcing them to share the decoder parameters. Please refer to (Ding, Yu, and Yang 2021) for details.¹ Given a full-modal

¹Note that our framework is model-agnostic and can be implemented with various non-FL multimodal segmentation models consisting of modality-specific encoders and modal fusion decoder(s) (e.g., Dorent et al. 2019; Shen and Gao 2019; Zhou et al. 2021). In

input X_M , each E_m first extracts features from the corresponding modality X_m , followed by D_M fusing multimodal features and generating segmentation masks. On the other hand, each single-modal client has a federated modality-specific encoder E_m and a personalized decoder D_m . E_m on the clients shares the same architecture as the server.

In each round of FL, the clients first receive parameters W_m^s from the server to replace its local copy W_m^i , where $i \in \{1, \dots, N_m\}$ and N_m is the number of clients with data of modality m , train for N_e epochs on local data, and then send updated W_m^i back to the server. After receiving W_m^i , the server averages W_m^i of the same modality (if $N_m > 1$): $W_m^s = \frac{1}{N_m} \sum_i W_m^i$, train for N_e epochs on the full-modal data, and sends updated W_m^s to the clients for the next round.² Thus, the server bridges the distribution gaps between modalities with the fusion decoder D_M and utilizes the complementary multimodal information to train each modality-specific encoder E_m via backpropagation.

Multi-Anchor Multimodal Representation: Besides aligning modality-specific encoders with the multimodal fusion decoder, the server also generates multi-anchor multimodal representations for the classes of interest, which will be distributed to the clients in addition to the encoder parameters. Liu et al. (2020) proposed communicating encoded representations, which may breach the privacy restriction. On the contrary, some works proposed to transmit category prototypes (Mu et al. 2023; Tan et al. 2022b). Yet a single prototype was highly compressed and may not carry enough representative information for a class, especially considering the significant inter-subject variations in 3D multimodal medical images.

In this work, we propose to extract *multiple* prototypes (Cui et al. 2020) from the fused multimodal features for each class of interest for enhanced representation power, which we refer to as anchors for their calibration purpose (Ning et al. 2021). Concretely, we extract per-class features from the fused multimodal feature maps of the decoder D_M by masked average pooling using the ground truth mask and apply the K-means method (MacQueen et al. 1967) to the extracted features to obtain N_k anchors. Intuitively, these N_k anchors are the modes of each class’s multimodal distribution. For the l^{th} feature scale level, where $l \in \{1, \dots, 4\}$ for the networks we use, the anchors for all the N_c classes can be collectively denoted by $A_l \in \mathbb{R}^{N_k N_c \times C_l}$, where C_l is the number of feature channels. Empirically, we determine the cluster membership using the most abstract feature level, i.e., $l = 4$, and apply the membership to compute $N_k = 3$ anchors for all levels (see corresponding experiments in the next section). This strategy can well preserve the full-modal information of each class while incurring little network

this work, we use (Ding, Yu, and Yang 2021) for demonstration due to its outstanding performance and straightforward architecture.

²We are aware of strategies for dynamic weight assignment for parameter aggregation based on clients’ data sizes (e.g., Hsu, Qi, and Brown 2020). Although this work focuses on inter-modal heterogeneity and assigns the same amount of data to all clients, we expect the incorporation of dynamic weight assignment to make our method more robust in practice.

Algorithm 1: FedMEMA algorithm. Note that the personalized (non-federated) decoder parameters are not shown below for simplicity.

Require: the modality set $M = \{\text{T1, T1c, T2, FLAIR}\}$ indexed by m , a full-modal training dataset \mathcal{D}_M on the server, the number of clients N_m with data of modality m , the monomodal training set \mathcal{D}_m^i on client i with data of modality m , the number of communication rounds N_r , and the number of training epochs N_e in each round.

Output: the collection of parameters $W_{\{m\}}^s = \{W_m^s\}$ for the modality-specific encoders, and the collection of multimodal anchors $A_{\{l\}} = \{A_l\}$ for different feature scale levels l (plus parameters of the personalized decoders).

- 1: **Server executes:**
- 2: Initialize $W_{\{m\}}^s$, and update $W_{\{m\}}^s$ by training on \mathcal{D}_M for N_e epochs
- 3: Initialize $A_{\{l\}}$ by K-means
- 4: **for** round $r = 1$ to N_r **do**
- 5: **for** $m \in M$ **do**
- 6: **for** each client $i \in N_m$ **do**
- 7: $W_m^i \leftarrow \text{ClientUpdate}(m, i, W_m^s, A_{\{l\}})$ \triangleright run on client i
- 8: $W_m^s = \frac{1}{N_m} \sum_i W_m^i$ \triangleright aggregate parameters for modality-specific encoder
- 9: Update $W_{\{m\}}^s$ by training on \mathcal{D}_M for N_e epochs
- 10: Update $A_{\{l\}}$ by exponential moving average
- 11: **ClientUpdate}(m, i, W_m^s, A_{\{l\}}):** \triangleright run on client i with modality m
- 12: $W_m^i \leftarrow W_m^s$
- 13: Update W_m^i by training on \mathcal{D}_m^i with LACCA (Eq. (1)) for N_e epochs
- 14: return W_m^i

transmission burden. It should also be noted that the few class-wise anchors are abstracted from the entire training population on the server, thus carrying little privacy information concerning individuals. To avoid the collapse of the training process due to jumps in cluster centroids as a result of re-clustering at each round (Xie, Girshick, and Farhadi 2016), we treat the anchors as a memory bank and update them smoothly via exponential moving average (EMA; Tarvainen and Valpola 2017): $\bar{a}_c = \omega \bar{a}_c + (1 - \omega) a_c$, where \bar{a}_c is an anchor for class c in the memory bank and updated by the closest cluster centroid a_c of the same class, and ω is set to 0.999 following Tarvainen and Valpola (2017).

Localized Adaptive Calibration via Cross-Attention:

In each federated round, the clients receive from the server the multimodal anchors A_l , which are used to calibrate local missing-modal representations. Concretely, denoting the final feature map at the l^{th} scale level of the encoder by $F_l \in \mathbb{R}^{\frac{D}{2^l} \times \frac{H}{2^l} \times \frac{W}{2^l} \times C_l}$, we reshape F_l to the dimension $\frac{DHW}{2^l 2^l 2^l} \times C_l$. Then, inspired by the attention operation in the Transformer architecture (Vaswani et al. 2017), we treat the reshaped F_l as queries and the multimodal anchors as the keys and values, and calibrate the local representations toward the global multimodal anchors by the cross attention:

$$F_l^{\text{cal}} = \text{Attn}(F_l, A_l) = \text{softmax}(F_l A_l^T / \sqrt{C_l}) A_l. \quad (1)$$

Number of anchors (N_k)	FLAIR	T1c	T1	T2	Avg	S
1	60.45±16.85*	75.34±22.02*	54.73±19.29	57.12±14.90*	61.91±14.74*	83.80±16.26*
2	60.22±15.61*	77.29±21.86*	57.66±18.21*	59.08±15.71*	63.56±14.63*	83.91±17.23*
3	62.52±16.79	76.37±21.83	57.26±17.24	60.36±17.23	64.13±15.17	84.17±17.19
4	61.16±16.87*	76.71±22.44*	56.28±16.56*	59.67±16.47*	63.45±14.93*	83.85±15.90*
5	59.91±17.72*	77.37±25.25*	57.21±16.97*	59.05±16.70*	63.38±16.09*	83.95±15.73*
7	60.93±17.83*	76.69±22.55*	57.84±18.21*	58.93±18.63*	63.60±15.64*	83.46±16.17*
Feature scale level (l)	FLAIR	T1c	T1	T2	Avg	S
1	59.58±16.33*	77.06±20.52*	56.63±18.46*	58.68±14.52*	62.99±14.55*	84.05±16.88*
2	61.15±16.54*	76.69±23.49*	56.12±18.37*	58.38±16.67*	63.08±15.74*	83.93±16.73
3	60.26±15.78*	77.10±22.03*	56.99±18.61*	58.77±15.70*	63.28±15.43*	83.21±16.19*
4	62.52±16.79	76.37±21.83	57.26±17.24	60.36±17.23	64.13±15.17	84.17±17.19
1-4	60.11±15.37*	75.99±23.95*	56.67±18.12	59.45±16.03*	63.05±15.42*	83.41±16.47*

Table 1: Results of experimental setting 1 on the *validation* set in mDSC (%). Top: varying N_k (number of multimodal anchors per class) with $l = 4$. Bottom: varying the feature scale level l (with $N_k = 3$) of the multimodal fusion decoder D_M , based on which the cluster membership is determined; $l = 4$ indicates the most abstract level of the smallest scale (i.e., at the bottleneck between the encoders and decoder), and “1-4” concatenates features of all four levels together for clustering. FLAIR, T1c, T1, and T2 indicate performance of the clients with the corresponding data modalities, Avg indicates their average, and “S” indicates server performance. *: $p < 0.05$ comparing against $N_k = 3$ (top) and $l = 4$ (bottom), respectively, in each column.

Finally, the calibrated features F_l^{cal} are reshaped back and element-wise added to the final features of the same scales of the decoder to participate in the subsequent forward propagation. The calibration process is localized and self-adaptive in that each client locally emphasizes the part of the global multi-anchor multimodal representations that best suits its own data modality and distributions—via the dot-product attention—to yield more powerful models tailored for itself. To this end, we name it the *localized adaptive calibration via cross-attention* (LACCA) module. The LACCA module is inserted in all four feature scales of our backbone networks. Note that the multimodal anchors are learnable parameters during FL and are directly used by the clients for inference after training. The complete algorithm of our method is detailed in Algorithm 1.

Experiments and Results

Dataset and Experimental Settings: We conduct experiments on the multimodal Brain Tumor Segmentation (BraTS) 2020 dataset (Menze et al. 2014; Bakas et al. 2018), which consists of 369 multi-contrast MRI scans with four sequences: T1, T1c, T2, and FLAIR. The goal is to segment three nested subregions of brain tumors: whole tumor, tumor core, and enhancing tumor. Following Ding, Yu, and Yang (2021), we divide the dataset into 219, 50, and 100 subjects for training, validation, and testing, respectively. The test set is used only for the final model evaluation, whereas the validation set is used for model optimization. Without loss of generality, we design two experimental settings per our problem definition.³ In setting 1, the training set is evenly divided among the server and four clients at random, i.e., no subject overlap between clients. Thus, the server and clients include 43, 44, 44, 44, and 44 training subjects, respectively. In setting 2, the server data remain unchanged, whereas the rest of the training data are randomly divided into 4+1 equal

³In this paper, we primarily focus on the inter-modal heterogeneity due to missing modalities but ignore the intramodal heterogeneity due to institutions, i.e., potential distribution discrepancies between data of the same modality but from different institutions.

parts where the additional “1” is the common data for all clients. The server and clients include 43, 71, 71, 71, and 71 training subjects, respectively. Meanwhile, the server and all clients in both settings use the same validation and test sets. Note that each client can only access the specific modalities of its assigned data. The mean of the Dice similarity coefficients (mDSC) of the three tumor subregions is employed as the evaluation metric, and the Wilcoxon signed rank test is used to analyze statistical significance.

Implementation: The proposed FL framework is implemented using PyTorch (1.13.0) and trained with five RTX 2080Ti GPUs, with the server on one GPU and the clients evenly distributed on the rest. We use the RFNet (Ding, Yu, and Yang 2021) as our server network, and its modality-specific encoder and regularizing decoder as the clients’ encoder and decoder, respectively. The LACCA module is implemented with eight attention heads. The input crop size is $80 \times 80 \times 80$ voxels, and the batch size is set to 1 and 3 for the server and clients, respectively. Other settings are the same for the server and clients. The commonly used Dice loss (Milletari, Navab, and Ahmadi 2016) plus the cross-entropy loss for medical image segmentation are employed. The Adam optimizer, with its learning rate and weight decay set to 0.0002 and 10^{-5} , respectively, is leveraged for optimization. We train the networks for 1000 rounds, and in each federated round, the server and clients are trained for one epoch. We follow Ding, Yu, and Yang (2021) for data preprocessing and augmentation. Our code is available at <https://github.com/QDaing/FedMEMA>.

Validating Designs for Multi-Anchor Multimodal Representations: Based on the validation data, we first determine 1) the optimal number of multimodal anchors per class (N_k) and 2) the optimal feature scale level l based on which the cluster membership is determined. We fix either of them to reduce the search space while varying the other. The results are shown in Table 1. Although the results look fairly stable, we select $N_k = 3$ and $l = 4$ for evaluation and comparison with other methods on the test data due to

Method	Setting 1					
	FLAIR	T1c	T1	T2	Avg	S
Local models	55.21±18.57*	64.60±25.13*	42.98±18.83*	54.84±16.78*	54.41±16.22*	79.91±16.48*
RFNet	54.65±18.07*	67.70±22.89*	43.69±16.92*	56.49±16.44*	55.63±15.43*	79.46±17.63*
FedAvg	54.04±17.48*	62.40±24.57*	36.60±14.71*	54.11±14.56*	51.78±14.17*	78.42±17.23*
PerFL	54.94±15.42*	63.56±26.13*	39.08±15.25*	53.57±15.09*	52.78±14.53*	78.71±16.80*
FedNorm	57.06±17.04*	68.45±21.13*	39.90±17.60*	56.16±16.56	55.39±15.64*	77.72±17.44*
CreamFL	55.07±16.42*	66.24±25.66*	47.01±18.30*	56.92±18.48*	56.31±16.01*	80.30±16.48*
FedMSplit	56.54±17.45*	69.58±22.56*	46.31±16.99*	59.96±15.20*	58.09±14.75*	81.01±15.93*
FedIoT	58.85±17.51*	71.14±21.01*	49.96±17.62*	61.07±15.29	60.25±15.22*	80.23±16.76*
FedMEMA (ours)	61.02±16.12	71.91±23.32	53.56±18.06	61.55±15.54	62.01±15.12	82.11±18.04
Method	Setting 2					
	FLAIR	T1c	T1	T2	Avg	S
Local models	55.35±19.06*	69.67±22.11*	44.24±19.87*	57.47±15.56*	56.68±15.73*	79.91±16.48*
RFNet	54.65±18.07*	67.70±22.89*	43.69±16.92*	56.49±16.44*	55.63±15.43*	79.46±17.63*
FedAvg	55.59±17.14*	65.47±23.11*	42.65±18.84*	56.61±18.22*	55.08±17.00*	78.19±16.83*
PerFL	56.70±16.09*	64.24±23.22*	45.16±17.01*	57.43±14.71*	55.88±15.73*	80.09±16.74
FedNorm	55.78±17.24*	70.91±22.11*	50.75±17.76*	51.80±16.12*	57.31±15.47*	78.28±17.44*
CreamFL	59.98±16.56*	69.54±23.70*	50.05±17.97*	59.55±17.16*	59.78±16.26*	81.55±15.22*
FedMSplit	58.87±16.26*	70.70±23.08*	50.41±17.10*	60.11±16.45*	60.02±15.09*	80.86±16.33
FedIoT	60.47±15.07*	71.96±21.20*	52.49±17.28	61.03±14.83*	61.48±14.64	81.47±17.31*
FedMEMA (ours)	62.84±16.17	73.49±21.77	56.46±19.04	61.58±14.87	63.59±15.27	83.27±17.27

Table 2: Experimental results on the *test* set in mDSC (%). FLAIR, T1c, T1, and T2 indicate the clients’ performance with the corresponding data modalities, Avg indicates their average, and “S” indicates server performance. *: $p < 0.05$ comparing against our method in each column.

Ablation	Server	Federated	LACCA	FLAIR	T1c	T1	T2	Avg	S
(a)	E&D	D	-	43.81±17.12*	48.83±25.13*	18.34±9.72*	43.59±18.10*	38.64±11.25*	80.05±15.46*
(b)	E&D	E	-	51.48±15.62*	58.51±17.17*	36.35±12.47*	47.97±17.06*	48.58±11.27*	81.11±16.38*
(c)	4E&D	4E	-	57.14±16.42*	72.95±14.66*	50.67±16.13*	58.01±17.12*	59.69±12.84*	82.11±16.42*
(d)	4E&D	4E	Mono-anchor	60.45±18.07*	75.34±22.89*	54.73±16.92	57.12±16.44*	61.91±15.43*	83.80±17.63*
(e) Ours	4E&D	4E	Multi-anchor	62.52±16.00	76.37±14.56	57.26±15.09	60.36±18.39	64.13±12.84	84.17±11.54

Table 3: Ablation study on the *validation* set in experimental setting 1 using mDSC (%). “E” and “D” are encoder and decoder, respectively. FLAIR, T1c, T1, and T2 indicate the clients’ performance with the corresponding data modalities, Avg indicates their average, and “S” indicates server performance. *: $p < 0.05$ comparing against our method in each column.

their highest performances in both the clients’ average and the server’s mDSCs compared with alternative values. We conjecture that $l = 4$ (i.e., the most abstract feature level) works the best due to its great capability of abstraction and denoising despite the relatively low resolution.

Comparison with Baseline and State-of-the-Art (SOTA)

Methods: We compare our proposed FedMEMA to various baseline and SOTA FL algorithms. As the baseline, the server and client models are trained locally on the private data of each site. As to SOTA FL algorithms, we adopt the classical FedAvg (McMahan et al. 2017) and several up-to-date approaches to FL on multimodal data or personalized models, including FedNorm (Bernecker et al. 2022), FedMSplit (Chen and Zhang 2022), CreamFL (Yu et al. 2023), FedIoT (Zhao, Barnaghi, and Haddadi 2022), and PerFL (Wang et al. 2019). Under the premise of keeping the methodological principles unchanged, necessary adaptations are made to ensure fair comparison: 1) for FedAvg and its derived methods (i.e., PerFL and FedNorm), which did not originally conduct server-end training, we make them do so on the server data as our method,⁴ and 2) we change Fe-

⁴Our preliminary experiments empirically showed that with the server-end training, they performed better than without it.

dIoT’s autoencoding clients to supervised networks. Also, we use the same networks as our clients’ for FedAvg and derivatives (in FedAvg infrastructure, the server and clients use the same networks) and the same networks as our server and clients for the counterparts in other methods. It should be noted that as CreamFL requires sharing the server data with all clients, it violates the privacy restriction in the medical context and increases the training data for the clients. Lastly, as RFNet (Ding, Yu, and Yang 2021) was originally designed for both full- and missing-modal segmentation after training with full-modal data, we also train it on the server data in its original recipe and evaluate its performance for comparison.

The results are shown in Table 2. As the comparative trends are similar in both settings, we mainly describe setting 1 below. Without modality-specific parameters, FedAvg and PerFL mostly yield worse performance than the baseline local models. This indicates that the inter-modal heterogeneity impedes the classical FL from effectively utilizing the extra data on the clients. By specializing the normalization parameters for different modalities, FedNorm achieves slight improvements in average mDSC across the clients but with slight to modest decreases in the server’s performance. The more complex and advanced CreamFL, FedM-

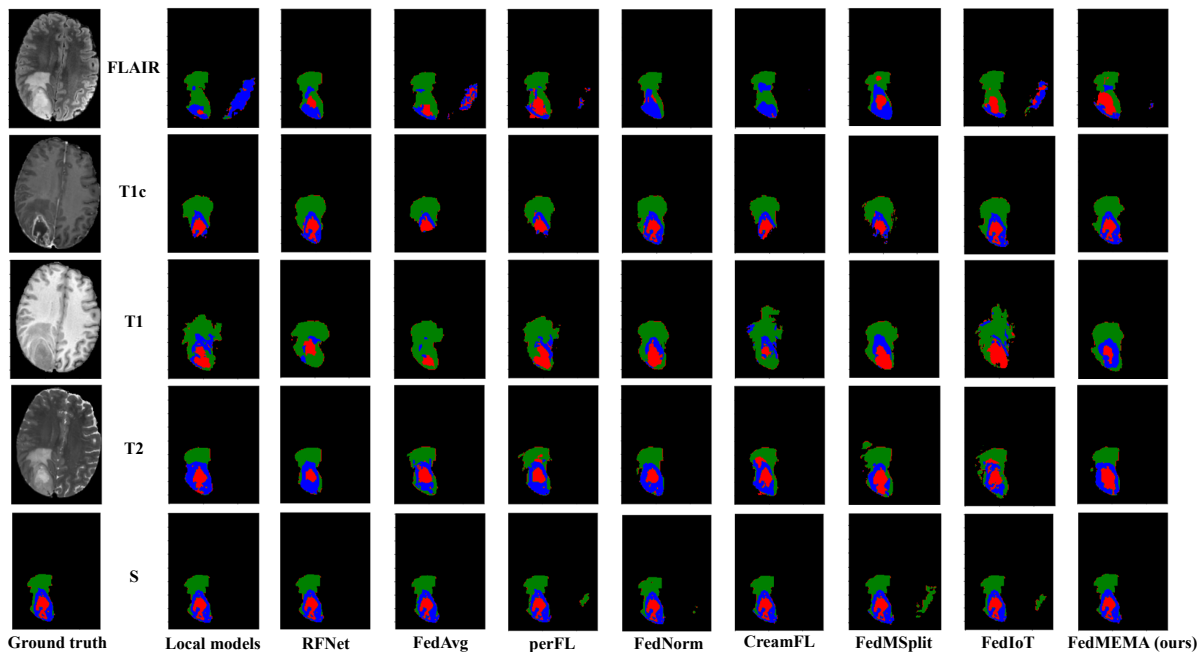


Figure 3: Example segmentation results in experimental setting 1 for a subject in the test set. FLAIR, T1c, T1, and T2 indicate the clients with the corresponding data modalities, and “S” indicates the server. Red: necrotic and non-enhancing tumor core, blue: enhancing tumor, and green: edema.

Split, and FedIoT frameworks can achieve comprehensive improvements over the baseline; especially, FedIoT exceeds in the clients’ average mDSC by close to 6%. In comparison, our FedMEMA further improves upon FedIoT by $\sim 2\%$ in both the clients’ average and server mDSCs and achieves the best performance for all clients and the server. We attribute our method’s advantages to the adaptive calibration via cross-attention between local monomodal and global full-modal representations. Remarkably, besides improving the clients’ performance with locally personalized models, FedMEMA also substantially enhances the server’s performance by effectively exploiting the clients’ data of heterogeneous modalities. Meanwhile, the RFNet, despite being a robust model for various missing-modal situations, yields performance comparable to the baseline local models, probably because it does not use the extra data on clients. Lastly, the performance in setting 2 is generally better than that in setting 1, likely due to the more training data available on each client. Fig. 3 shows example segmentation results.

Ablation Study: We conduct thorough ablation studies to validate the efficacy of our novel framework design, including the federated modality-specific encoders and personalized decoders, the LACCA module, and the multi-anchor multimodal representations. The results are presented in Table 3, where the first two rows are variants of the classical FedAvg (McMahan et al. 2017) with either the encoder or decoder federated, and the last three are variants of our proposed method. It can be seen that, among the variants of FedAvg, federating the encoder while personalizing the decoder (row (b)) outperforms the reverse (row (a)). On top of

that, our modality-specific encoders (row (c)) achieve substantial performance boosts over the FedAvg family, e.g., the clients’ average mDSC improves by $\sim 11\%$ compared with row (b), demonstrating the effectiveness of the FL architecture in our problem setting. Row (d) additionally incorporates the LACCA module but with mono-anchor representations obtained by averaging all server data, achieving further improvements, especially on the clients ($>2\%$ in average mDSC). This suggests that multimodal representations are effective for the adaptive calibration of local monomodal features. The last row is our full model with multi-anchor representations, yielding the best performances in both average missing-modal mDSC across the clients ($\sim 64\%$) and full-modal mDSC on the server ($\sim 84\%$). These results indicate that multiple anchors represent the 3D multimodal medical data better than the mono ones, as expected.

Conclusion

In this paper, we proposed FedMEMA—a new FL framework with federated modality-specific encoders and multimodal anchors for brain tumor segmentation in multi-parametric MRI with missing-modal clients, and demonstrated its superior performance to existing FL methods on the public BraTS 2020 benchmark in the extreme case of monomodal clients. In future work, we plan to evaluate FedMEMA with the more common settings of hetero-modal clients and more datasets. In addition, this paper mainly focused on the inter-modal heterogeneity due to missing modalities but ignored the intramodal heterogeneity due to institutions, which was a limitation. We also plan to consider both types of heterogeneities together in the future.

Acknowledgments

This work was supported in part by the National Key R&D Program of China under Grant 2020AAA0109500/2020AAA0109501, and in part by the National Natural Science Foundation of China (Grant No. 62371409).

References

- Adnan, M.; Kalra, S.; Cresswell, J. C.; Taylor, G. W.; and Tizhoosh, H. R. 2022. Federated learning and differential privacy for medical image analysis. *Scientific Reports*, 12(1): 1953.
- Azad, R.; Khosravi, N.; and Merhof, D. 2022. SMU-Net: Style matching U-Net for brain tumor segmentation with missing modalities. In *International Conference on Medical Imaging with Deep Learning*, 48–62. PMLR.
- Bakas, S.; et al. 2018. Identifying the best machine learning algorithms for brain tumor segmentation, progression assessment, and overall survival prediction in the BRATS challenge. *arXiv preprint arXiv:1811.02629*.
- Bercea, C. I.; Wiestler, B.; Rueckert, D.; and Albarqouni, S. 2021. FedDis: Disentangled federated learning for unsupervised brain pathology segmentation. *arXiv preprint arXiv:2103.03705*.
- Bernecker, T.; Peters, A.; Schlett, C. L.; Bamberg, F.; Theis, F.; Rueckert, D.; Weiß, J.; and Albarqouni, S. 2022. FedNorm: Modality-based normalization in federated learning for multi-modal liver segmentation. *arXiv preprint arXiv:2205.11096*.
- Chen, H.; Qin, Z.; Ding, Y.; Tian, L.; and Qin, Z. 2020. Brain tumor segmentation with deep convolutional symmetric neural network. *Neurocomputing*, 392: 305–313.
- Chen, J.; and Zhang, A. 2022. FedMSplit: Correlation-adaptive federated multi-task learning across multimodal split networks. In *Proceedings of the 28th ACM SIGKDD Conference on Knowledge Discovery and Data Mining*, 87–96.
- Chen, S.; Ding, C.; and Liu, M. 2019. Dual-force convolutional neural networks for accurate brain tumor segmentation. *Pattern Recognition*, 88: 90–100.
- Cui, H.; Wei, D.; Ma, K.; Gu, S.; and Zheng, Y. 2020. A unified framework for generalized low-shot medical image segmentation with scarce data. *IEEE Transactions on Medical Imaging*, 40(10): 2656–2671.
- Ding, Y.; Gong, L.; Zhang, M.; Li, C.; and Qin, Z. 2020. A multi-path adaptive fusion network for multimodal brain tumor segmentation. *Neurocomputing*, 412: 19–30.
- Ding, Y.; Yu, X.; and Yang, Y. 2021. RFNet: Region-aware fusion network for incomplete multi-modal brain tumor segmentation. In *Proceedings of the IEEE/CVF International Conference on Computer Vision*, 3975–3984.
- Dorent, R.; Joutard, S.; Modat, M.; Ourselin, S.; and Vercauteren, T. 2019. Hetero-modal variational encoder-decoder for joint modality completion and segmentation. In *Medical Image Computing and Computer Assisted Intervention*, 74–82. Springer.
- Hsu, T.-M. H.; Qi, H.; and Brown, M. 2020. Federated visual classification with real-world data distribution. In *Computer Vision—ECCV 2020: 16th European Conference, Glasgow, UK, August 23–28, 2020, Proceedings, Part X 16*, 76–92. Springer.
- Hu, M.; et al. 2020. Knowledge distillation from multi-modal to mono-modal segmentation networks. In *Medical Image Computing and Computer Assisted Intervention—MICCAI 2020: 23rd International Conference, Lima, Peru, October 4–8, 2020, Proceedings, Part I 23.*, 772–781. Springer.
- Iv, M.; Yoon, B. C.; Heit, J. J.; Fischbein, N.; and Wintermark, M. 2018. Current clinical state of advanced magnetic resonance imaging for brain tumor diagnosis and follow up. In *Seminars in Roentgenology*, volume 53, 45–61. Elsevier.
- Kaissis, G. A.; Makowski, M. R.; Rückert, D.; and Braren, R. F. 2020. Secure, privacy-preserving and federated machine learning in medical imaging. *Nature Machine Intelligence*, 2(6): 305–311.
- Li, T.; Sahu, A. K.; Talwalkar, A.; and Smith, V. 2020. Federated learning: Challenges, methods, and future directions. *IEEE Signal Processing Magazine*, 37(3): 50–60.
- Liu, F.; Wu, X.; Ge, S.; Fan, W.; and Zou, Y. 2020. Federated learning for vision-and-language grounding problems. In *Proceedings of the AAAI Conference on Artificial Intelligence*, volume 34, 11572–11579.
- MacQueen, J.; et al. 1967. Some methods for classification and analysis of multivariate observations. In *Proceedings of the Fifth Berkeley Symposium on Mathematical Statistics and Probability*, volume 1, 281–297. Oakland, CA, USA.
- McMahan, B.; Moore, E.; Ramage, D.; Hampson, S.; and y Arcas, B. A. 2017. Communication-efficient learning of deep networks from decentralized data. In *Artificial Intelligence and Statistics*, 1273–1282. PMLR.
- Menze, B. H.; Jakab, A.; Bauer, S.; Kalpathy-Cramer, J.; Farahani, K.; Kirby, J.; Burren, Y.; Porz, N.; Slotboom, J.; Wiest, R.; et al. 2014. The multimodal brain tumor image segmentation benchmark (BRATS). *IEEE Transactions on Medical Imaging*, 34(10): 1993–2024.
- Milletari, F.; Navab, N.; and Ahmadi, S.-A. 2016. V-Net: Fully convolutional neural networks for volumetric medical image segmentation. In *Fourth International Conference on 3D Vision*, 565–571. IEEE.
- Mu, X.; Shen, Y.; Cheng, K.; Geng, X.; Fu, J.; Zhang, T.; and Zhang, Z. 2023. FedProc: Prototypical contrastive federated learning on non-IID data. *Future Generation Computer Systems*, 143: 93–104.
- Myronenko, A. 2018. 3D MRI brain tumor segmentation using autoencoder regularization. In *Brainlesion: Glioma, Multiple Sclerosis, Stroke and Traumatic Brain Injuries: 4th International Workshop, BrainLes 2018, Held in Conjunction with MICCAI 2018, Granada, Spain, September 16, 2018, Revised Selected Papers, Part II 4.*, 311–320. Springer.
- Ning, M.; Lu, D.; Wei, D.; Bian, C.; Yuan, C.; Yu, S.; Ma, K.; and Zheng, Y. 2021. Multi-anchor active domain adaptation for semantic segmentation. In *Proceedings of the*

- IEEE/CVF International Conference on Computer Vision*, 9112–9122.
- Shen, Y.; and Gao, M. 2019. Brain tumor segmentation on MRI with missing modalities. In *Information Processing in Medical Imaging*, 417–428. Springer.
- Tan, A. Z.; Yu, H.; Cui, L.; and Yang, Q. 2022a. Towards personalized federated learning. *IEEE Transactions on Neural Networks and Learning Systems*.
- Tan, Y.; Long, G.; Liu, L.; Zhou, T.; Lu, Q.; Jiang, J.; and Zhang, C. 2022b. FedProto: Federated prototype learning across heterogeneous clients. In *Proceedings of the AAAI Conference on Artificial Intelligence*, volume 36, 8432–8440.
- Tarvainen, A.; and Valpola, H. 2017. Mean teachers are better role models: Weight-averaged consistency targets improve semi-supervised deep learning results. *Advances in Neural Information Processing Systems*, 30: 1195–1204.
- Vaswani, A.; Shazeer, N.; Parmar, N.; Uszkoreit, J.; Jones, L.; Gomez, A. N.; Kaiser, Ł.; and Polosukhin, I. 2017. Attention is all you need. *Advances in Neural Information Processing Systems*, 30: 5998–6008.
- Wang, K.; Mathews, R.; Kiddon, C.; Eichner, H.; Beaufays, F.; and Ramage, D. 2019. Federated evaluation of on-device personalization. *arXiv preprint arXiv:1910.10252*.
- Wang, Y.; Zhang, Y.; Liu, Y.; Lin, Z.; Tian, J.; Zhong, C.; Shi, Z.; Fan, J.; and He, Z. 2021. ACN: Adversarial co-training network for brain tumor segmentation with missing modalities. In *Medical Image Computing and Computer Assisted Intervention—MICCAI 2021: 24th International Conference, Strasbourg, France, September 27–October 1, 2021, Proceedings, Part VII 24.*, 410–420. Springer.
- Xie, J.; Girshick, R.; and Farhadi, A. 2016. Unsupervised deep embedding for clustering analysis. In *International Conference on Machine Learning*, 478–487. PMLR.
- Xiong, B.; Yang, X.; Qi, F.; and Xu, C. 2022. A unified framework for multi-modal federated learning. *Neurocomputing*, 480: 110–118.
- Yan, B.; Wang, J.; Cheng, J.; Zhou, Y.; Zhang, Y.; Yang, Y.; Liu, L.; Zhao, H.; Wang, C.; and Liu, B. 2021. Experiments of federated learning for COVID-19 chest X-ray images. In *Advances in Artificial Intelligence and Security*, 41–53. Springer International Publishing.
- Yan, Z.; Wicaksana, J.; Wang, Z.; Yang, X.; and Cheng, K.-T. 2020. Variation-aware federated learning with multi-source decentralized medical image data. *IEEE Journal of Biomedical and Health Informatics*, 25(7): 2615–2628.
- Yu, Q.; Liu, Y.; Wang, Y.; Xu, K.; and Liu, J. 2023. Multi-modal federated learning via contrastive representation ensemble. In *The Eleventh International Conference on Learning Representations*.
- Zhao, Y.; Barnaghi, P.; and Haddadi, H. 2022. Multimodal federated learning on IoT data. In *IEEE/ACM Seventh International Conference on Internet-of-Things Design and Implementation*, 43–54. IEEE.
- Zhou, C.; Ding, C.; Wang, X.; Lu, Z.; and Tao, D. 2020. One-pass multi-task networks with cross-task guided attention for brain tumor segmentation. *IEEE Transactions on Image Processing*, 2020, 29: 4516–4529., 29: 4516–4529.
- Zhou, T.; Canu, S.; Vera, P.; and Ruan, S. 2021. Latent correlation representation learning for brain tumor segmentation with missing MRI modalities. *IEEE Transactions on Image Processing*, 30: 4263–4274.

Supplementary Material: Federated Modality-specific Encoders and Encoders and Multimodal Anchors for Personalized Brain Tumor Segmentation

Methods	Whole tumor						Tumor core						Enhancing tumor					
	FLAIR	T1c	T1	T2	Avg	S	FLAIR	T1c	T1	T2	Avg	S	FLAIR	T1c	T1	T2	Avg	S
Local models	79.84	61.39	64.14	78.12	70.87	87.15	54.07	68.87	43.32	54.89	55.29	<u>82.46</u>	31.73	63.55	21.48	31.51	37.07	70.13
RFNet	79.40	66.78	65.06	80.25	72.87	87.01	56.42	72.89	45.14	57.69	58.04	81.92	28.11	63.44	20.87	31.53	35.99	69.44
FedAvg	79.09	64.13	60.73	78.14	70.52	86.54	52.52	64.88	38.96	55.24	52.90	78.59	30.52	58.19	10.12	28.96	31.94	70.13
PerFL	81.03	63.30	55.94	76.68	69.24	86.86	53.44	66.74	42.02	53.72	53.98	79.90	30.34	60.65	19.27	30.31	35.14	69.38
FedNorm	80.50	65.29	52.63	76.99	68.85	85.64	57.49	70.86	44.81	57.71	57.72	79.43	31.73	63.55	21.48	31.51	37.07	70.13
CreamFL	82.07	64.91	<u>68.81</u>	80.59	74.10	87.99	54.25	69.15	48.17	55.68	56.81	82.05	33.19	<u>69.21</u>	22.25	33.78	39.61	70.85
FedMSplit	82.15	68.14	68.33	<u>82.37</u>	75.25	88.69	56.67	73.25	48.80	58.68	56.81	82.05	30.81	67.34	21.82	35.85	38.96	<u>72.03</u>
FedIoT	82.03	<u>70.98</u>	68.47	<u>81.28</u>	<u>75.69</u>	87.71	<u>59.86</u>	<u>76.50</u>	<u>52.68</u>	<u>63.59</u>	63.16	81.50	<u>34.67</u>	65.93	<u>28.72</u>	<u>38.34</u>	<u>41.92</u>	71.49
Ours	84.26	71.49	71.37	82.88	77.50	89.48	61.39	<u>74.37</u>	<u>57.23</u>	<u>63.43</u>	64.11	84.29	37.41	69.87	32.09	38.34	44.43	72.57

Table S1: Class-wise results in mDSC (%) of different tumor subregions for the setting-1 results shown in Table 2. The local models are trained locally on the private data of each site. FLAIR, T1c, T1, and T2 indicate the clients’ performance with the corresponding data modalities, Avg indicates their average, and “S” indicates server performance.

Method	FLAIR ¹	T1c ¹	T1 ¹	T2 ¹	FLAIR ²	T1c ²	T1 ²	T2 ²	Avg	S
Local models	40.66±16.60*	38.47±16.76*	41.97±16.33*	42.14±18.83*	36.12±15.99*	38.52±18.47*	38.39±17.90*	35.88±15.31*	39.02±15.29*	79.91±16.48*
RFNet	54.65±18.07*	67.70 ±22.89*	43.69±16.92*	56.49±16.44*	54.65±18.07*	67.70 ±22.89*	43.69±16.92*	<u>56.49</u> ±16.44*	<u>55.63</u> ±15.43*	79.46±17.63*
FedAvg	51.29±18.28*	56.04±28.51*	32.78±15.72*	51.45±15.99*	49.90±17.95*	59.48±25.72*	34.04±15.49*	50.04±15.99*	48.13±14.40*	76.31±17.88*
PerFL	50.24±18.37*	55.54±29.23*	33.49±14.87*	51.70±15.70*	52.41±16.80	59.54±26.74*	34.62±14.79*	51.88±16.82*	48.68±15.12*	75.66±16.35*
FedNorm	49.81±14.63*	59.84±27.32*	31.19±14.06*	46.95±14.29*	49.87±15.07*	59.99±28.55*	28.63±13.28*	49.55±15.34*	46.98±13.11*	76.38±18.83*
CreamFL	<u>56.23</u> ±16.96	65.46±24.33*	43.27±15.99*	53.39±16.59*	50.57±16.66*	63.45±26.66*	40.59±17.02*	50.83±16.83*	52.97±14.34*	80.40±15.62*
FedMSplit	45.30±16.22*	63.64±27.78*	<u>45.29</u> ±16.18*	50.73±14.48*	44.08±15.50*	63.86±26.73*	43.96±16.54	55.41±14.07*	51.53±14.18*	80.96±16.51*
FedIoT	55.18±16.69*	67.55±23.51	44.56±15.95*	<u>58.17</u> ±14.42*	52.52±16.22	67.39±25.92*	47.13 ±18.12*	50.60±16.81*	55.39±15.10*	<u>81.77</u> ±16.32*
Ours	56.81 ±15.72	<u>67.65</u> ±25.96	46.48 ±14.84	59.04 ±14.82	54.78 ±17.36	68.45 ±24.38	<u>47.05</u> ±15.46	58.29 ±16.53	57.32 ±14.55	82.31 ±16.74

Table S2: Experimental results on the *test* set in mDSC (%) with *eight clients*. The local models are trained locally on the private data of each site. The compared methods are RFNet (Ding, Yu, and Yang 2021), FedAvg (McMahan et al. 2017), PerFL (Wang et al. 2019), FedNorm (Bernecker et al. 2022), CreamFL (Yu et al. 2023), FedMSplit (Chen and Zhang 2022), and FedIoT (Zhao, Barnaghi, and Haddadi 2022). FLAIR^{1,2}, T1c^{1,2}, T1^{1,2}, and T2^{1,2} indicate the performance of the clients with the corresponding data modalities, Avg indicates their average, and “S” indicates server performance. *: $p < 0.05$ comparing against our method in each column.

More Results

Subregional Performance: In Table S1, we provide class-wise results of different tumor subregions for the setting-1 results shown in Table 2.

Performance with Eight Monomodal Clients: We conduct a more challenging experiment with eight clients, two for each of the four modalities, i.e., $N_m = 2$ for $m \in \{T1, T1c, T2, FLAIR\}$. Concretely, we keep the server’s training data the same as setting 1 in Table 2 and evenly distribute the rest training data to the clients. The results are shown in Table S2. Compared to Table 2, both the clients’ and server’s performances drop due to the more challenging setting, as expected. Despite that, the comparative trends are similar. Notably, our method performs best in both the clients’ average and the server’s mDSCs. In addition, it also yields the highest mDSCs for six of eight clients and the second-highest for the rest two clients. These results further confirm the efficacy of our method in federated learning for medical image analysis in the presence of inter-modal heterogeneity due to missing modalities.

Performance with Bi- and Tri-modal Clients: Our proposed FedMEMA framework can be readily extended to other application scenarios, including the more common ones of multimodal clients. The extension is straightforward: for a multimodal client, we only need to employ a modality-specific encoder for each of its modalities and a fusion decoder—similar to the server. For proof of concept, we experiment with bi- and tri-modal clients here. Concretely, we keep the server’s training data the same as setting 1 in Table 2 and evenly distribute the rest of the training data to the clients. Given four modalities, there can be six and four different combinations of two and three modalities, respectively. Therefore, we use six and four clients in the bi- and tri-modal settings, respectively. The results in Table S3 show that our method is consistently effective for bi- and tri-modal clients.

Performance with More Heterogeneous Multimodal Scenario: Next, we experiment with a more heterogeneous multimodal scenario where the number of modalities varies for clients: two clients have one modality (FLAIR and T1c),

Bimodal	Local models	FedAvg	CreamFL	FedMSplit	FedIoT	Ours
Avg	64.12±15.42*	63.38±14.83*	64.02±15.53*	69.81±15.34*	65.12±14.93*	70.61 ±15.23
S	79.91±16.48*	78.92±23.38*	80.53±22.30*	79.75±22.11*	80.75±22.83	81.07 ±23.53
Trimodal	Local models	FedAvg	CreamFL	FedMSplit	FedIoT	Ours
Avg	72.45±16.16*	71.74±15.16*	73.23±17.15*	77.5±15.30	75.49±15.36*	77.64 ±15.15
S	79.91±16.48*	79.51±23.43*	79.46±17.63*	80.18±22.13*	81.82±22.22	81.84 ±22.43

Table S3: Experimental results on the *test* set in mDSC (%) with bi- and tri-modal clients. The local models are trained locally on the private data of each site. Avg indicates the clients’ average performance and “S” indicates server performance. *: $p < 0.05$ comparing against our method.

	Loc. models	FedAvg	CreamFL	FedMSplit	FedIoT	Ours
Avg	60.54±14.89*	56.47±15.03*	63.48±15.74*	64.72±15.81*	64.26±15.12*	67.26 ±15.34
S	79.91±16.48*	77.72±24.98*	79.95±23.14*	80.42±22.08*	81.37±22.66	81.98 ±22.68

Table S4: Experimental results on the *test* set in mDSC (%) with more heterogeneous clients: two clients have one modality (FLAIR and T1c), and the other two have two (T1&T2 and FLAIR&T1), with no patient overlap. The local models are trained locally on the private data of each site. Avg indicates the clients’ average performance and “S” indicates server performance. *: $p < 0.05$ comparing against our method.

	Local models	FedAvg	CreamFL	FedMSplit	FedIoT	Ours
Avg	48.72±15.77*	41.07±12.76*	38.03±17.71*	46.27±12.89*	51.68±15.13	52.94 ±14.43
S	79.18±15.45*	72.78±20.02*	79.40±15.38*	78.79±16.22*	80.56±14.87	80.71 ±15.02

Table S5: Experimental results on BraTS 2018 (Bakas et al. 2018) in mDSC (%) following setting 1 in the main text. The local models are trained locally on the private data of each site. Avg indicates the clients’ average performance and “S” indicates server performance. *: $p < 0.05$ comparing against our method.

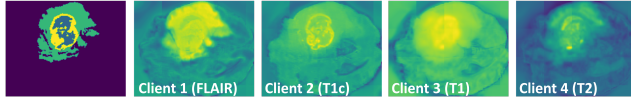


Figure S1: Client-wise cross-attention, i.e., $F_i A_i^T$ in Eq. (2). The first column shows the subregional tumor mask.

and the other two have two (T1&T2 and FLAIR&T1), with no patient overlap. The results in Table S4 demonstrate the advantages of our method over others in the more heterogeneous scenario.

Performance on Alternative Dataset: Following the literature (e.g., Ding et al. 2021), we use BraTS 2018 (Bakas et al. 2018) as an alternative dataset and present the additional results (corresponding to setting 1 in Table 2) in Table S5. We can see that the superior performance of our method persists.

Client-wise Cross-Attention: In the ablation study, rows (d) and (e) in Table 3 demonstrated that our proposed localized adaptive calibration via cross-attention (LACCA) brought substantial performance improvements. Here, we further visualize the client-wise cross-attention (i.e., $F_i A_i^T$ in Eq. (2)) in Fig. S1, where the four clients attend to distinct tumor regions in accordance with their modalities.